

Interferometric Phase and Coherence of Forest Estimated by ESPRIT-based Polarimetric SAR Interferometry

Hiroyoshi Yamada¹, Koichi Sato¹, Yoshio Yamaguchi¹, Wolfgang.-M. Boerner²

1: Faculty of Engineering, Niigata University
Ikarashi 2-8050, Niigata 950-2181, Japan

Tel/Fax: +81-25-262-7477, e-mail: yamada@ie.niigata-u.ac.jp

2: University of Illinois at Chicago
UIC-EECS/CSN, m/c 154, SEL 4210
900 West Taylor Street, IL 60607-7018, USA

Abstract—Polarimetric SAR interferometry has been widely studied for forest observations. The technique utilizes polarization state difference among local scattering centers of the forest to decompose them. Using the method, we can estimate precise forest parameters. We proposed an alternative method based on the ESPRIT algorithm for the estimation. The method can detect as many as 3 local scatterers with fully polarimetric data, and can extract interferometric phase of each local scatterer. In this paper, we verify the availability of the method in 2- and 3-local-scatterer model for forest estimation, and show that forest analysis with 3-local-scatterer improve height estimation accuracy. SIR-C/X-SAR data were used for these verifications. In addition, experimental results of restricted dual-polarization data are also provided to show availability of the method.

I. INTRODUCTION

Recently many researches have proposed for biomass estimation using polarimetric and interferometric approach [1]-[3]. Polarimetric SAR interferometry [2], [3] is the most promising technique for forest parameter extraction. However, inversion technique in [3] requires multiple parameter least-square estimation whose complexity is high, and often becomes ill-condition.

Authors have proposed an alternate polarimetric SAR interferometry based on the ESPRIT [4] (Estimation of Signal Parameters via Rotational Invariance Technique) [5], [6]. The method enables us to resolve interferometric phase of local scatterers without inversion, and can detect scattering centers as many as paired-channels. This means that we can detect as many as 3 phases for fully polarimetric observation, and 2 for dual polarimetric observation.

In this paper, we show the validity of the method to illustrate the relation between interferometric phases by the ESPRIT and complex coherence by the conventional polarimetric SAR interferometry. The used experimental data sets were the SIR-C/X-SAR data of the Tien-Shan test-site. Estimated results in restricted dual polarization data set are also provided to show availability of the method.

II. COHERENCE MODEL OF FOREST

In the forest observation at L-Band, both ground and canopy back scattering are contained in the received signals. When canopy scattering is assumed to be random dipole volume scattering, complex coherence of the forest can be

modeled as[1][3]

$$\tilde{\gamma}(\omega) = e^{j\phi_0} \frac{\tilde{\gamma}_V + m(\omega)}{1 + m(\omega)}, \quad (1)$$

where ϕ_0 is an underlying topographic phase, and $\tilde{\gamma}_V$ is a complex coherence corresponding to volume scattering. $m(\omega)$, where ω expresses unitary scattering mechanism, denotes amplitude ratio of ground to volume scattering.

Eq.(1) can be also written as

$$\tilde{\gamma}(\omega) = e^{j\phi_0} \left[\tilde{\gamma}_V + \frac{m(\omega)}{1 + m(\omega)} (1 - \tilde{\gamma}_V) \right]. \quad (2)$$

This equation means that the complex coherence in any polarization combination appear on a straight line between $\tilde{\gamma}_V e^{j\phi_0}$ and $e^{j\phi_0}$. By its extremes, $m = \infty, 0$, we can derive coherence of volume and ground scatterings (Fig.1). To estimate these parameters using the polarimetric SAR interferometry [3], fully polarimetric data are necessary.

III. ESPRIT ALGORITHM

Assuming repeat pass observation in the forest scattering, there exist two or more dominant scattering centers. The main two scattering centers locate on ground and in canopy. Thus the observed signals in kl - polarization (e.g., HH, HV, VH and VV) in orbit-1 and 2 can be given by

$$E_1^{(kl)} = \sum_{i=1}^d \sigma_i s_i^{(kl)} e^{j\frac{\Delta\rho_i}{\lambda} \rho} + n_1^{(kl)} \quad (3a)$$

$$E_2^{(kl)} = \sum_{i=1}^d \sigma_i s_i^{(kl)} e^{j\frac{\Delta\rho_i}{\lambda} (\rho + \Delta\rho)} + n_2^{(kl)} \quad (3b)$$

where d and $\sigma_i s_i^{(kl)}$ denote the number of dominant scattering centers and backscattered component of the i -th scattering center in kl polarization, respectively. ρ and $\Delta\rho_i$ denotes slant-range distance and path-difference of the i -th local scatterer. n is additive noise. Rewriting (3a) and (3b) in matrix-vector notation, we can obtain:

$$E_1 = [E_1^{(HH)}, E_1^{(HV)} E_1^{(VV)}]^T = S\sigma + n_1 \quad (4a)$$

$$E_2 = [E_2^{(HH)}, E_2^{(HV)} E_2^{(VV)}]^T = SD\sigma + n_2 \quad (4b)$$

This is an example for 3-polarization (HH, HV, VV) observation. Note that above expressions hold in any

polarization data sets including dual polarization observation. Phase of the i -th Element in the diagonal matrix \mathbf{D} is the interferometric phase of the i -th local scatterer.

The problem formulated in (4a) and (4b) has the same form as those of Direction-of-Arrival estimation with array by the ESPRIT [4]. See [5] and [6] for the details of the method for polarimetric SAR interferometry application.

The algorithm can directly estimate \mathbf{D} without knowing \mathbf{S} and σ , and can also eliminate noise bias automatically. They are the advantages for the conventional method. Furthermore, the method can detect scattering centers as many as the number of polarization channels. This means we can detect 3 local scattering centers for fully polarimetric observation, and 2 for dual-polarization observation.

IV. EXPERIMENTAL RESULTS

The used data are L-Band single-look complex (SLC) image pair of the Tien-Shan test-site by the SIR-C/X-SAR system on October 8 and 9, 1994 (data takes 122.20 & 154.20). The total power image is shown in Fig.3. The HH, HV and VV data are used for fully polarimetric analysis, therefore, we can detect 2 local scattering centers corresponding to ground and canopy plus 1 local scattering center between them at maximum. The evaluation patches in the following experiments were also shown in Fig.2.

Figs. 4(a) and (b) show the interferometric phases estimated by the ESPRIT algorithm assuming two dominant scattering centers ($d = 2$) and three scattering centers ($d = 3$), respectively. Complex coherence described in Sec.II are also plotted. The values, $opt.1-3$, are the optimized coherence used in the polarimetric SAR interferometry[3]. It is clear that these coherences are almost located on the line. Then the model in Sec.II holds in this area. The phase ‘ESPRIT.1’ and ‘ESPRIT.2’ in Fig.4(a) show the phases of ground and canopy, respectively. Geometrical relation of the phases and coherences agree well with those shown in Fig.1. The estimated phases in Fig.2(a) seems to be slightly biased. This may be caused by the spatial distribution of scattering center. Point scatterers are assumed in the ESPRIT, therefore, bias will appear for highly distributed local scatterers. When we apply the ESPRIT with $d = 3$, another scattering center appears and phase estimation accuracy for ground and canopy is improved.

Estimated results of another patch are shown in Fig.5. The estimated phases with $d = 2$ contain large bias. In this patch, spatial/height distribution of the canopy scattering center(s) may be widely distributed so that the bias is caused. In such a case, phase estimation with $d = 3$ is effective to improve phase accuracy (Fig.5(b)).

When there exist only two dominant scattering centers, as shown in Fig.3, we can apply the ESPRIT based polarimetric SAR interferometry with dual-polarization data set. Estimation results with dual polarization data sets are shown in Figs.6 (a)-(c). The estimated phases with VV-HV data sets are almost the same as those in Fig.4. In this case,

ground component in HH and HV channel seems to be small because of dense forest. As the results, dual-polarization estimation including VV data set derives the good estimation results. Suitable polarization pair for forest estimation will depend on its condition (e.g. dense or sparse). This will be considered in near future.

V. CONCLUSIONS

In this paper, we show relation of the estimated interferometric phase of local scattering centers by the ESPRIT and complex coherence by the polarimetric SAR interferometry. Experimental results well agrees with that derived by the coherence model of forest. In addition, we show estimation performance of the ESPRIT with restricted dual-polarization data set. Estimation performance will depend on forest conditions, however, the method can help us to analyze forest SAR data with dual-polarization data set such as fine-mode of ALOS/PALSAR.

In this paper, we only show experimental results of SIR-C/X-SAR, space-borne SAR data. This method is also available for air-borne SAR data. Results of E-SAR data will be also shown in the presentation.

REFERENCES

- [1] R.N.Treuhft and P.R.Siqueria, “Vertical structure of vegetated land surfaces from interferometric and polarimetric radar,” *Radio Science*, vol.35, no.1, pp.141-177, Jan-Feb. 2000.
- [2] S.R.Cloud and K.P.Papathanassiou, “Polarimetric SAR interferometry,” *IEEE Trans. Geosci. Remote Sensing*, vol.36, no.5, pp.1551-1565, Sept. 1998.
- [3] K.P.Papathanassiou and S.R.Cloud, “Single-baseline polarimetric SAR interferometry,” *IEEE Trans.Geosci. Remote Sensing*, vol.39, no.11,pp.2352-2363, Nov. 2001.
- [4] R.Roy and T.Kailath, “ESPRIT -Estimation of signal parameters via rotational invariance techniques,” *IEEE Trans. Acoust., Speech and Signal Processing*, vol.37, no.7, pp.984-995, July 1989.
- [5] H.Yamada, *et al.*, “Polarimetric SAR interferometry for forest analysis based on the ESPRIT algorithm,” *IEICE Trans. Electron.*, vol.E84-C, no.12, pp.1917-1924, Dec. 2001.
- [6] H.Yamada, *et al.*, “Polarimetric SAR interferometry for forest canopy analysis by using the super-resolution method,” *Proc. IGRASS 2001*, Sydney, Australia, July 2001.

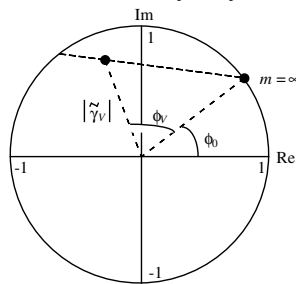


Fig.1 Geometrical representation of the coherence model.

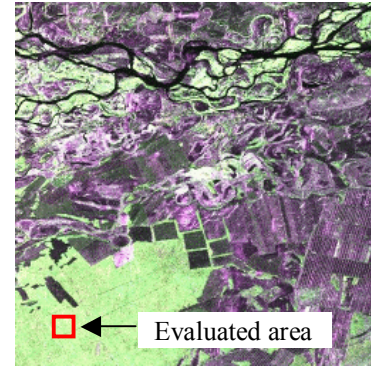
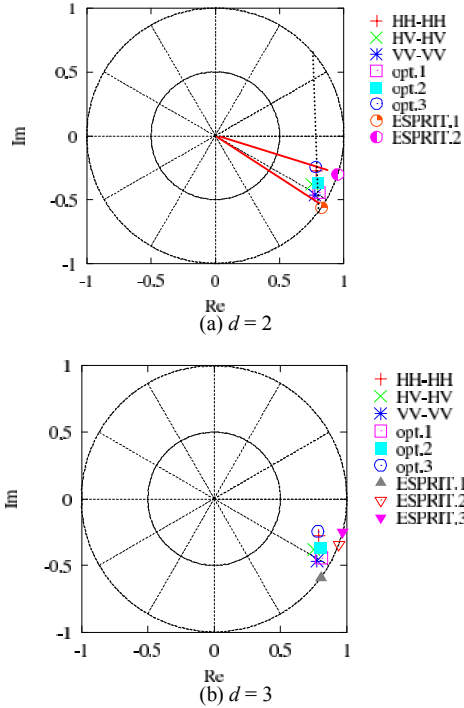


Fig.2 L-Band total power image of the Tien-Shan flight-path.

Fig.3 Distribution of the complex coherence of the conventional method and interferometric phases estimated by the ESPRIT algorithm at patch 1.

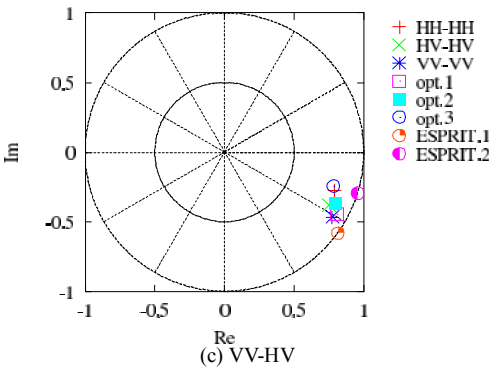
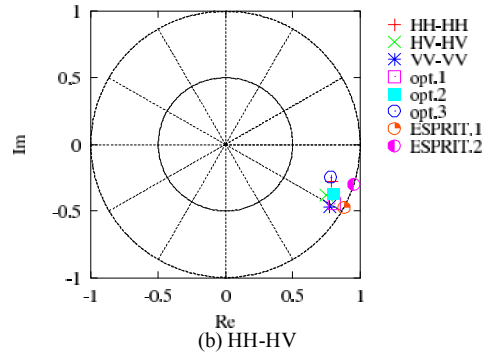
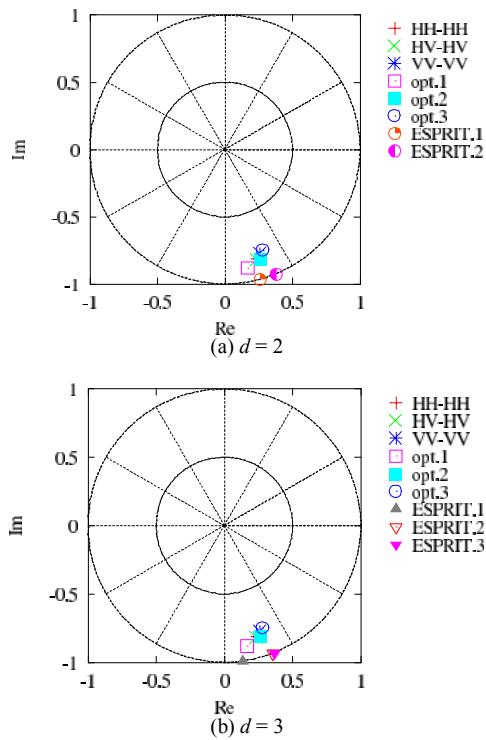
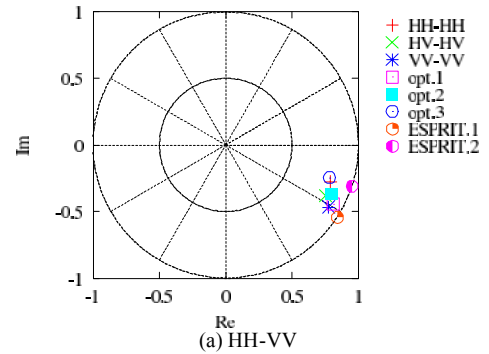


Fig.4 Distribution of the complex coherence of the conventional method and interferometric phases estimated by the ESPRIT algorithm at patch 2.

Fig.5 Distribution of the complex coherence of the conventional method (3-pol. case) and interferometric phases estimated by the ESPRIT algorithm with dual-polarization data sets at patch 1.